ADVANCED FUNCTIONAL MATERIALS

www.afm-journal.de

Metal–Organic Frameworks

On page 3855, J. Pérez-Ramírez and co-workers demonstrate the reconstruction of water-degraded HKUST-1, one of the most studied metal–organic frameworks, by means of facile, one-step, solvent-assisted treatments. This regeneration process is symbolized by the phoenix, the long-lived bird from Greek mythology that obtains new life by arising from the ashes of its predecessor. Marcel Reich (marcelreich.com) is acknowledged for creating the lovely cover artwork.

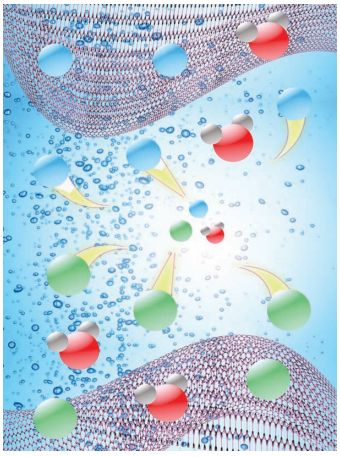

Water Treatment

Capacitive deionization (CDI) is a competent water desalination technique offering an appropriate route to obtain clean water. On page 3917, Y.-M. Yan, K.-N. Sun and co-workers design and prepare a 3D-structured, graphene-based electrode using sponge (polyurethane, PU) as a template. The electrode possesses a large surface area, wide pore size distribution from nanopores to micropores, and low internal resistance, therefore exhibiting a remarkable electrosorptive capacity of 4.95 mg g^{-1} and a desorption rate of 25 min.

Magnetite

Strong uniaxial shape anisotropy in magnetosome chains is explored in magnetotactic bacteria using 2D X-ray diffraction to determine the crystallographic orientation of the magnetosomes relative to the chain axis. On page 3926, D. Faivre and co-workers reveal [111] and [100] fiber textures along the chain direction, with the [100] axis appearing unfavorable as a magnetic hard axis in magnetite. Calculations show how this can be turned into an effective easy axis for a given particle elongation.

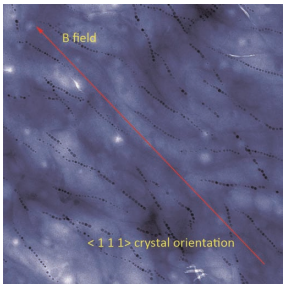

FULL PAPERS

Biomedical Sensors

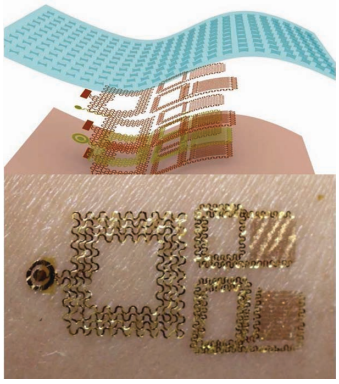

An ultrathin, stretchable device capable of soft lamination onto the surface of the skin for wireless measurements of dielectric and surface strain properties is presented. The device uses LC resonators with capacitive electrodes to qualify the skin properties, and is capable of conformal and spontaneous skin integration.

Metal–Organic Frameworks

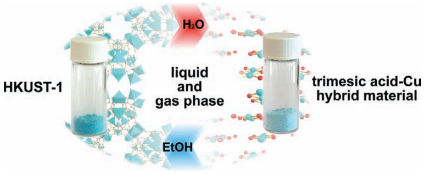

Reconstruction of water-degraded HKUST-1 back into the original material is demonstrated through solvent-assisted liquid- and gas-phase treatments. Up to 94% porosity and 85% CO_2 sorption capacity could be recovered from a completely collapsed metal–organic framework. The degradation routes affect the physicochemical features and the kinetics of reconstruction. This method opens promising directions for the large-scale application of these materials.

Actuators

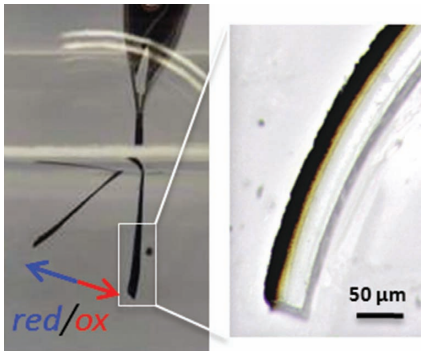

Durable, biocompatible materials capable of controlled movements are sought after for a variety of drug delivery, surgical, and tissue engineering applications. Methods to synthesize films composed of an interpenetrating network of the biopolymer silk fibroin and poly(pyrrole) are described, and the ability of these materials to function as electromechanical actuators in a biologically relevant environment are demonstrated.

Gene Therapy

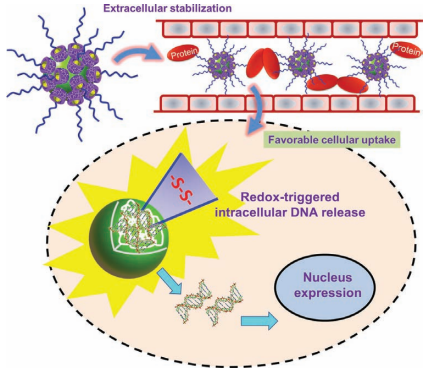

A convenient supramolecular strategy is demonstrated for building a highly efficient multifunctional gene carrier system. The system is self–assembled and integrated from two polymeric building blocks via host-guest interaction between β-cyclodextrin and adamantyl moieties, possessing the functions of disulfide bond based reduction-responsive degradation, and zwitterionic phosphorylcholine based extracellular stabilization and favorable cellular uptake.

FULL PAPERS

Electrical properties of MFU-4 and Co-MFU-4 metal-organic frameworks are investigated by temperature-dependent broad-band dielectric and optical spectroscopy. Density functional theory calculations performed for framework and cluster model compounds give a detailed picture of the frameworks' electronic structures and confirm experimental band gap values. The combined results enable a systematic engineering of MFU-4-type semiconducting microporous materials.

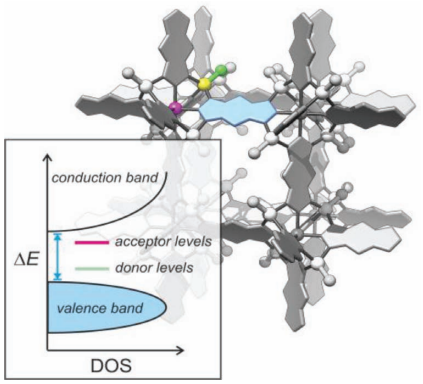

Coordination Polymers

Near-infrared quantum rods (QRs) with tunable emission and aspect ratio are synthesized as nano-platforms for engineering multifunctional nanoprobes. The as-prepared QRs exhibit great stability and little nonspecific binding. Paramagnetic gadolinium ions can be easily assembled on the QRs to produce multifunctional contrast agents for in vivo lymph node fluorescence and magnetic resonance dual-modal imaging. It provides a general method for designing rod-shape multifunctional nanostructure.

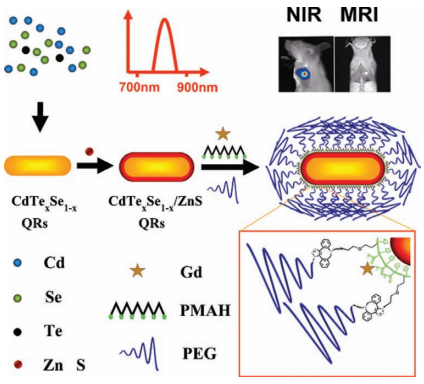

Semiconductor Nanocrystals

Guard flow-enhanced organic vapor jet printing technique enables additive patterning of organic thin films in air, without the use of solvents. During deposition in air, ambient oxygen and moisture are incorporated in the film's "wing" region. This work relates the degree of air exposure to pentacene film's morphology and electronic properties via synchrotron X-ray diffraction and thin-film transistor measurements, respectively.

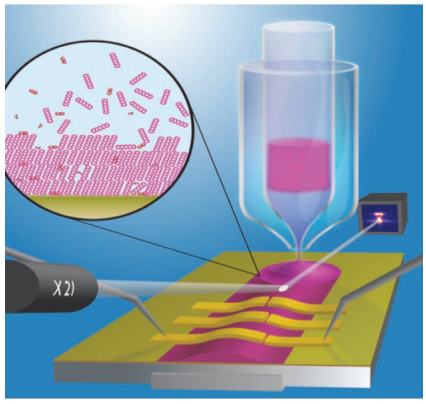

Organic Electronics

Sponge-templated graphene sheets (STGS) with high specific surface area, wide pore size distribution, and low internal resistance are prepared through a simple annealing method. The as-prepared STGS exhibits promising CDI performance with an ultrahigh electrosorptive capacity of 4.95 mg g^{-1} and fast desorption rate of 25 min.

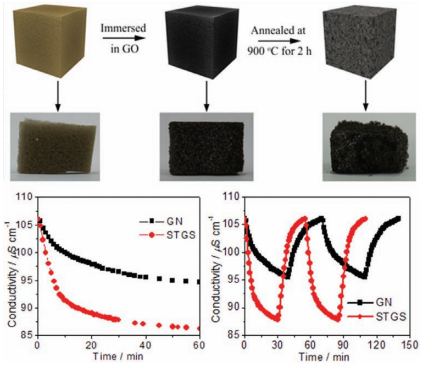

Water Treatment

CONTENTS

FULL PAPERS

Magnetite

Magnetite Crystal Orientation in Magnetosome Chains

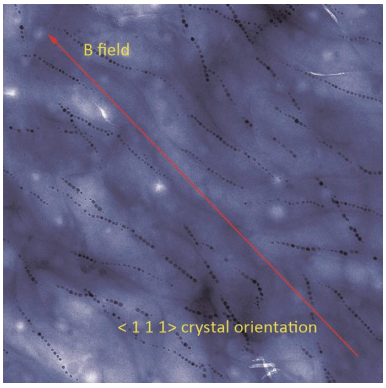

2D-X-ray diffraction analyses of aligned magnetotactic bacteria reveal [111] and [100] fiber textures along the chain direction as a function of cell species. The [100] axis appears unfavorable because it represents a magnetic hard axis in magnetite. Calculations show how this can be turned into an effective easy axis for a given particle elongation.

Composite Hydrogels

A Novel Wound Dressing Based on Ag/Graphene Polymer Hydrogel: Effectively Kill Bacteria and Accelerate Wound Healing

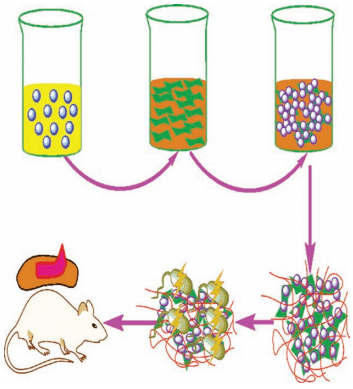

A novel application range of graphene hydrogel in wound dressing is exploited. The hydrogels are composed of Ag–graphene composite, AA, and BIS. When the mass ratio of Ag to graphene is 5:1, the hydrogel (Ag5G1) shows strong antibacterial activity, large swelling ratio, excellent biocompatibility, and good extensibility, and it can significantly accelerate the healing rate of artificial wounds in rats.

Anodic Materials

Synthesis, Structure Transformation, and Electrochemical Properties of Li_2MgSi as a Novel Anode for Li-Ion Batteries

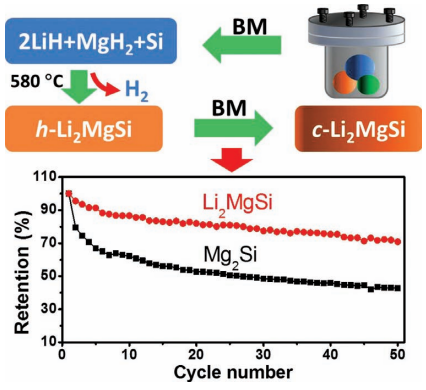

A novel hexagonal Li_2MgSi is successfully synthesized through a hydrogen-driven chemical reaction technique, which exhibits significantly improved cycling stability with respect to that of Mg_2Si as an anode material for Li-ion batteries. Ball milling induces a polymorphic transformation of Li_2MgSi from the hexagonal phase to the cubic phase and further improves the electrochemical lithium storage properties.

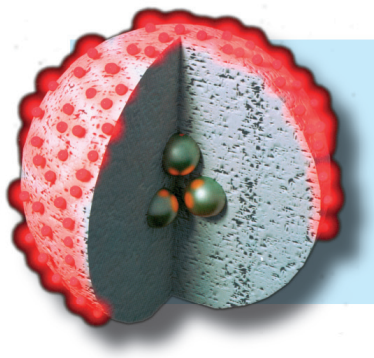

How to contact us:

Editorial Office:
Phone: (+49) 6201-606-286/531
Fax: (+49) 6201-606-500
Email: afm@wiley-vch.de

Reprints:
cherth@wiley-vch.de

Copyright Permission:
Fax: (+49) 6201-606-332
Email: rights@wiley-vch.de

FULL PAPERS

An asymmetric supercapacitor based on nitrogen-doped porous carbon networks and 3D flower-like MnO_2 as the negative and positive electrode materials, respectively, exhibits a considerably high energy density of 63 Wh kg^{-1} and an excellent cycling performance with 92% specific capacitance retention after 5000 cycles. Those results offer a low-cost, eco-friendly design of electrode materials for high-performance supercapacitors.

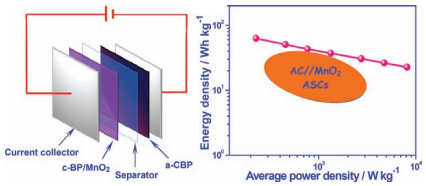

Asymmetric Supercapacitors

Resistive switching of (001) epitaxial multiferroic $BiFeO_3/La_{0.67}Sr_{0.33}MnO_3/SrTiO_3$ heterostructures is investigated for varying lengths scales in both the thickness and lateral directions. Macroscale current–voltage analyses in conjunction with local conduction atomic force microscopy reveal that whilst both the local and global resistive states are strongly driven by polarization direction, the type of conduction mechanism is different for each distinct thickness regime.

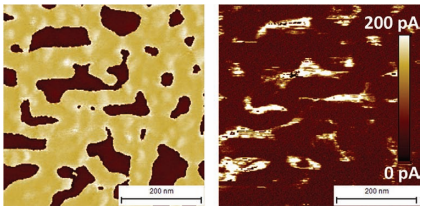

Multiferroic Heterostructures

High quantum efficiency above 25% in thermally activated delayed fluorescence device is achieved using mixed hosts without any exciplex formation between host materials. A combination of mCP and BmPyPb is effective to improve the quantum efficiency up to 28.6%.

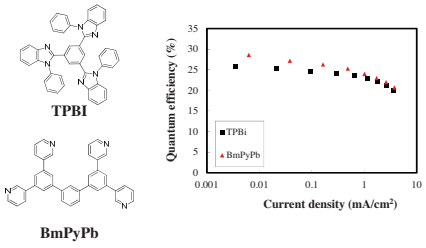

Organic Electronics

Thermal degradation near operating temperatures occurs at the metal-organic interface if the polymer T_g is near the operating temperature. The degradation is reversed by peeling off and reapplying the metal electrode. X-ray photoelectron spectroscopy measurements reveal a larger amount of polymer adheres to electrodes peeled from aged devices than electrodes peeled from fresh devices. Using an inverted device suppresses degradation.

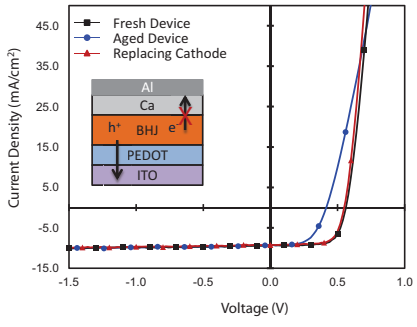

Organic Photovoltaics

FULL PAPERS

Solar Cells

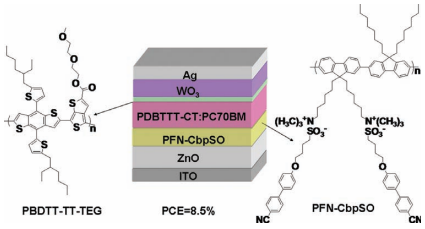

Solution processed polymer solar cell with outstanding efficiency and stability is fabricated at room temperature. Spin-coating conjugated polyelectrolyte-ionic liquid-crystal complex at cathode and tungsten oxide together with ter(ethyleneoxide)-substituted PBDTT-TT-TEG at anode achieves optimized efficiency 7.8%, which further increases to 8.5% after inserting ZnO as cathode interlayer. This is best PCE for PBDTTT-C-T:$PC_{70}BM$-based cells with solution processed interlayers reported to date

Superconductors

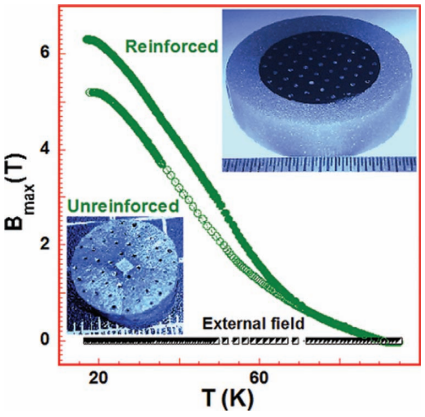

High-performance $YBa_2Cu_3O_{7-\delta}$ bulk superconductors with improved reliability and thermal transfer ability are fabricated in short time. The approach taken here is based on the insertion of a metal wires network into the holes of $YBa_2Cu_3O_{7-\delta}$ drilled single grains progressively annealed at high temperature under oxygen pressure. The achieved microstructure is pore-free and crack-free, and the thermal exchange markedly fosters inside the superconductor.

Gas Sensors

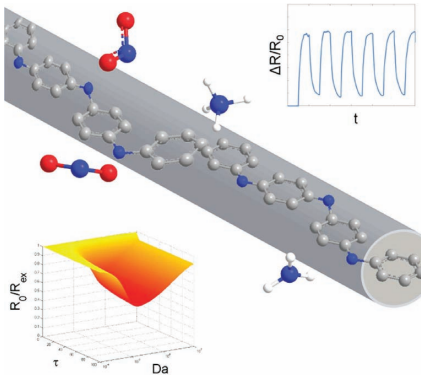

Electrospun polyaniline fibers are fabricated and evaluated as chemiresistive gas sensors. The fibers exhibit remarkable changes in measured resistances for ammonia and nitrogen dioxide sensing, with short characteristic response times. A time-dependent reaction-diffusion model is used to extract physical parameters from fitting experimental data, and to illustrate the selection of optimal material design parameters for gas sensing by nanofibers.